Awake Hippocampal Sharp-Wave Ripples Support Spatial Memory

Shantanu P. Jadhav, **Caleb Kemere**, **P. Walter German**, and **Loren M. Frank**[*]

Department of Physiology and Center for Integrative Neuroscience, University of California, San Francisco, CA 94143, USA

Abstract

The hippocampus is critical for spatial learning and memory. Hippocampal neurons in awake animals exhibit place field activity that encodes current location, as well as sharp-wave ripple (SWR) activity during which representations based on past experiences are often replayed. The relationship between these patterns of activity and the memory functions of the hippocampus is poorly understood. We interrupted awake SWRs in animals learning a spatial alternation task. We observed a specific learning and performance deficit that persisted throughout training. This deficit was associated with awake SWR activity, as SWR interruption left place field activity and post-experience SWR reactivation intact. These results provide a link between awake SWRs and hippocampal memory processes, which suggests that awake replay of memory-related information during SWRs supports learning and memory-guided decision-making.

Animals use past experience to guide decisions, an ability that requires storing memories for the events of daily life and retrieving those memories as needed. This storage and retrieval depends on the hippocampus and associated structures in the medial temporal lobe (1–5), but the specific patterns of neural activity that support these memory functions remain poorly understood. We know that during exploration, individual neurons fire in specific regions of space (5, 6) known as place fields. In contrast, during periods of slow movement, immobility, and slow-wave sleep, groups of neurons are active during sharp-wave ripple (SWR) events (7, 8). This activity frequently represents a replay of a past experience on a rapid time scale (9–13). SWRs that occur during sleep contribute to memory consolidation of preceding experiences (14–18), and both changes in place fields and the intensity of awake memory reactivation have been correlated with memory performance (19). Awake SWRs in particular can reactivate sets of place fields encoding forward and reverse paths associated with both current and past locations (9–13). This reactivation has been hypothesized to contribute to multiple functions including learning, retrieval, consolidation,

and trajectory planning (19–23). To investigate the role of awake hippocampal SWRs and to determine whether awake replay can be functionally dissociated from place field activity, we selectively disrupted awake SWRs in rats learning a hippocampus-dependent W-track task (24). We have previously shown that the hippocampus frequently replays memories of past experience while animals learn this task (11).

Animals are rewarded on the W-track each time they visit the end of one of the three maze arms in the correct task sequence (center-left-center-right-center…, Fig. 1A). This task consists of two components: (i) an "outbound" alternation component that specifies that when the animal is in the center arm, the next correct outer arm is the one opposite to the outer arm it most recently visited, and (ii) an "inbound" return-to-center component that specifies that when the animal is in an outer arm, it must then proceed to the center arm. Hippocampal damage impairs the rapid learning of both components, although hippocampal-lesion animals eventually learn the task (24), which suggests that other structures such as the basal ganglia and prefrontal cortex can support task performance after extended training.

We disrupted awake hippocampal SWRs on the W-track across 8 days of learning with the use of an online feedback system similar to that used in previous studies that disrupted SWRs during post-behavior sleep (17, 18). SWRs in CA1 were detected by monitoring power in the ripple band (25) simultaneously across multiple tetrodes. Online detection of a SWR event triggered calibrated single-pulse electrical stimulation of CA3 afferents to CA1 delivered through a bipolar stimulation electrode in the ventral hippocampal commissure (vHC, fig. S1). This terminated the ripple oscillation within 25 ms of SWR onset and transiently inhibited CA1 spiking (Fig. 1, B to E, and fig. S2) (25). We calibrated the stimulation magnitude for each animal to find the minimum current that inhibited multiunit spiking activity in CA1 for ~100 ms (Fig. 1, C to E, and fig. S2). To ensure that any observed effects were due to disruption of activity during SWRs, we used the same online detection protocol in a control group of animals, but delayed stimulation by 150 to 200 ms after detection (17) (Fig. 1, B and E, and fig. S2). This control stimulation left SWR-associated spiking activity intact while still inhibiting a temporally equivalent period of hippocampal activity (Fig. 1E).

Animals in three groups—SWR disruption, control stimulation, and an unimplanted, unstimulated group (n = 6, 4, and 4, respectively)—ran two 15-min sessions on the W-track with interleaving 15-min rest sessions (one "pre" rest session before behavior and two "post" rest sessions after behavior) each day (Fig. 1F) for a total of 8 days. Spiking activity in CA1 was monitored during all run and rest sessions in the SWR disruption and control stimulation groups. To control for the possibility that vHC stimulation could lead to changes in the synaptic strength of CA3 input to CA1, we also measured evoked field responses to 0.1-Hz probe stimulation in the intervening rest periods (Fig. 1F) (25).

SWR disruption animals were impaired on the outbound component of the task as compared to controls (Fig. 2, A to D). SWR disruption animals performed a lower proportion of correct outbound trials than the control animals across all eight days of learning (Fig. 2A; n = 6, 4, and 4 animals, repeated-measures ANOVA, main effect of group, $P < 0.001$, group $\times$

day interaction, $P < 0.01$; no differences between control and unstimulated group, Ps > 0.4). We also used a state-space model to estimate the trial and day on which performance was above chance for each animal (24–26) (Fig. 2B and figs. S3 to S5). SWR disruption animals learned later than controls in terms of both trials and days to criterion (Fig. 2C, rank-sum test, Ps < 0.01). SWR disruption animals also had significantly lower performance levels on the final 2 days (Fig. 2D, rank-sum test, $P < 0.01$). Further, all SWR disruption animals learned more slowly than all eight control animals, and all SWR disruption animals had lower performance on days 7 and 8 than all eight control animals. These perfect separations in the rank order of learning rates and final performance would occur by chance with a probability < 0.0007. Similar statistical results were obtained with the two control groups combined (25).

In contrast, SWR disruption animals performed normally in the inbound component of the task (Fig. 2E; n = 6, 4, and 4 animals, repeated-measures ANOVA, main effect of group, P > 0.33, group × day interaction, $P > 0.5$) and had similar learning rates as compared to controls (Fig. 2F and figs. S6 to S8). Learning trial and day were similar among the SWR disruption and control groups (Fig. 2G, rank-sum tests, Ps > 0.5), and the final performance levels achieved by the animals in the last 2 days were also similar (Fig. 2H, rank-sum test, P > 0.48). The distinction between learning on the outbound and inbound tasks remained clear when learning curves were aligned by trial number for the three groups (fig. S9).

SWR disruption effectively suppressed hippocampal activity during SWRs but had no discernible effect on place cell representations. We examined the stability of CA1 place fields in run sessions (Fig. 3A and fig. S10) and computed the correlation between linearized place fields (11, 25, 27) of each cell across the two run sessions within each day (Fig. 3, A and B, and fig. S11). We found no difference in place field stability between place cells from the two groups (SWR disruption: n = 108 place cells, mean correlation = 0.80 ± 0.02; control stimulation: n = 96 cells, mean correlation = 0.81 ± 0.02; t test, P > 0.5) across all days (Fig. 3B; two-way ANOVA, main effect of group, P > 0.16, group × day interaction, P > 0.5; within-day comparisons, n.s.; Bonferroni post hoc tests). The distributions of peak rates and place field sizes for the two groups were also similar (Fig. 3, C and D; KS test, Ps > 0.5). We also found no evidence that stimulation induced synaptic plasticity. We found no difference in field postsynaptic potential (PSP) slopes in response to 0.1-Hz probe stimulation between the pre rest period before behavior and the post rest periods after behavior compared on each day for all animals (example and Z scores across all days in Fig. 3E, n.s., t test, P > 0.43). Further, differences in other behavior or stimulation parameters could not account for the learning deficit in the SWR disruption group. (figs. S12 to S17).

The deficit on outbound but not inbound trials suggests that loss of awake SWRs did not cause a global deficit in memory consolidation. Consistent with this, we found no evidence for alteration of the rest/sleep SWR activity associated with consolidation. Pairs of cells with overlapping place fields had theta-modulated correlations during run periods and showed increased correlations during SWRs in post relative to pre rest periods (Fig. 4A), as has been observed in animals with intact hippocampal activity (14, 16, 28). For both SWR disruption and control stimulation groups, reactivation strength (Fig. 4B) was significantly correlated with place field overlap (linear regression, Ps < 0.001) and with correlations during run (fig.

S18; linear regression, Ps < 0.001). SWR rates in the rest periods were also similar for the SWR disruption and control stimulation groups (Fig. 4C and fig. S18).

Our observation of intact place fields, intact reactivation during rest SWRs, and intact inbound performance suggests that place fields and post-experience reactivation are sufficient to support learning and performance of the inbound trials. As hippocampal lesions disrupt learning on the inbound component, place cell activity may be important for learning and applying the inbound rule. More broadly, place cell activity could provide information about current position that promotes rapid learning and application of location-specific rules (fig. S19).

The specific performance deficit observed in SWR disruption animals provides a causal link between awake hippocampal SWRs and the spatial memory requirements of outbound trials. Learning of the outbound rule requires linking immediate and more remote past experience to reward (fig. S19), and the observed replay of both recent and remote experiences during awake SWRs (11–13) is well suited to contribute to this learning. Applying the outbound rule in the center arm requires knowledge of current location, memory for immediate past outer arm location, and the ability to use that memory to plan and execute a movement to the opposite outer arm. This memory-guided decision-making process has been referred to as "spatial working memory" (2, 4). Impaired outbound performance in the SWR disruption group on later days (Fig. 2), even after most animals performed above chance, suggests a spatial working memory impairment. Additional evidence for this was provided by a decline in performance in three of the animals from the control stimulation group that were switched to SWR disruption on days 9 and 10 (fig. S20). Forward and backward replay of both past and possible future trajectories during SWRs (9–13, 21) may therefore contribute to outbound performance. Conversely, we would predict that manipulations that cause selective spatial working memory deficits, such as the removal of parvalbumin-positive interneurons in CA1 and GluR1 knockout animals at the CA3-CA1 synapse (29, 30), have their impact primarily as a result of disrupting awake replay processes. Thus, we hypothesize that the forward and reverse replay of local and spatially remote paths seen during awake replay provides information about past locations and possible future options (fig. S19) to structures such as the prefrontal cortex that use this information to learn the outbound alternation rule and to subsequently apply the learned rule to guide behavior.

Supplementary Material

Refer to Web version on PubMed Central for supplementary material.

Acknowledgments

References and Notes

1. Squire LR. Psychol Rev. 1992; 99:195. [PubMed: 1594723]
2. Eichenbaum, H.; Cohen, NJ. From Conditioning to Conscious Recollection. Oxford Univ. Press; New York: 2001.

3. Riedel G, et al. Nat Neurosci. 1999; 2:898. [PubMed: 10491611]

4. Olton DS, Becker JT, Handelmann GE. Behav Brain Sci. 1979; 2:313.

5. O'Keefe, J.; Nadel, L. The Hippocampus as a Cognitive Map. Oxford Univ. Press; London: 1978.

6. Wilson MA, McNaughton BL. Science. 1993; 261:1055. [PubMed: 8351520]

7. Buzsáki G. Brain Res. 1986; 398:242. [PubMed: 3026567]

8. O'Neill J, Senior T, Csicsvari J. Neuron. 2006; 49:143. [PubMed: 16387646]

9. Foster DJ, Wilson MA. Nature. 2006; 440:680. [PubMed: 16474382]

10. Diba K, Buzsáki G. Nat Neurosci. 2007; 10:1241. [PubMed: 17828259]

11. Karlsson MP, Frank LM. Nat Neurosci. 2009; 12:913. [PubMed: 19525943]

12. Davidson TJ, Kloosterman F, Wilson MA. Neuron. 2009; 63:497. [PubMed: 19709631]

13. Gupta AS, van der Meer MA, Touretzky DS, Redish AD. Neuron. 2010; 65:695. [PubMed: 20223204]

14. Wilson MA, McNaughton BL. Science. 1994; 265:676. [PubMed: 8036517]

15. Buzsáki G. Cereb Cortex. 1996; 6:81. [PubMed: 8670641]

16. Kudrimoti HS, Barnes CA, McNaughton BL. J Neurosci. 1999; 19:4090. [PubMed: 10234037]

17. Girardeau G, Benchenane K, Wiener SI, Buzsáki G, Zugaro MB. Nat Neurosci. 2009; 12:1222. [PubMed: 19749750]

18. Ego-Stengel V, Wilson MA. Hippocampus. 2010; 20:1. [PubMed: 19816984]

19. Dupret D, O'Neill J, Pleydell-Bouverie B, Csicsvari J. Nat Neurosci. 2010; 13:995. [PubMed: 20639874]

20. O'Neill J, Pleydell-Bouverie B, Dupret D, Csicsvari J. Trends Neurosci. 2010; 33:220. [PubMed: 20207025]

21. Carr MF, Jadhav SP, Frank LM. Nat Neurosci. 2011; 14:147. [PubMed: 21270783]

22. Singer AC, Frank LM. Neuron. 2009; 64:910. [PubMed: 20064396]

23. Cheng S, Frank LM. Neuron. 2008; 57:303. [PubMed: 18215626]

24. Kim SM, Frank LM. PLoS ONE. 2009; 4:e5494. [PubMed: 19424438]

25. See supplementary materials on *Science* Online.

26. Smith AC, et al. J Neurosci. 2004; 24:447. [PubMed: 14724243]

27. Dragoi G, Harris KD, Buzsáki G. Neuron. 2003; 39:843. [PubMed: 12948450]

28. O'Neill J, Senior TJ, Allen K, Huxter JR, Csicsvari J. Nat Neurosci. 2008; 11:209. [PubMed: 18193040]

29. Reisel D, et al. Nat Neurosci. 2002; 5:868. [PubMed: 12195431]

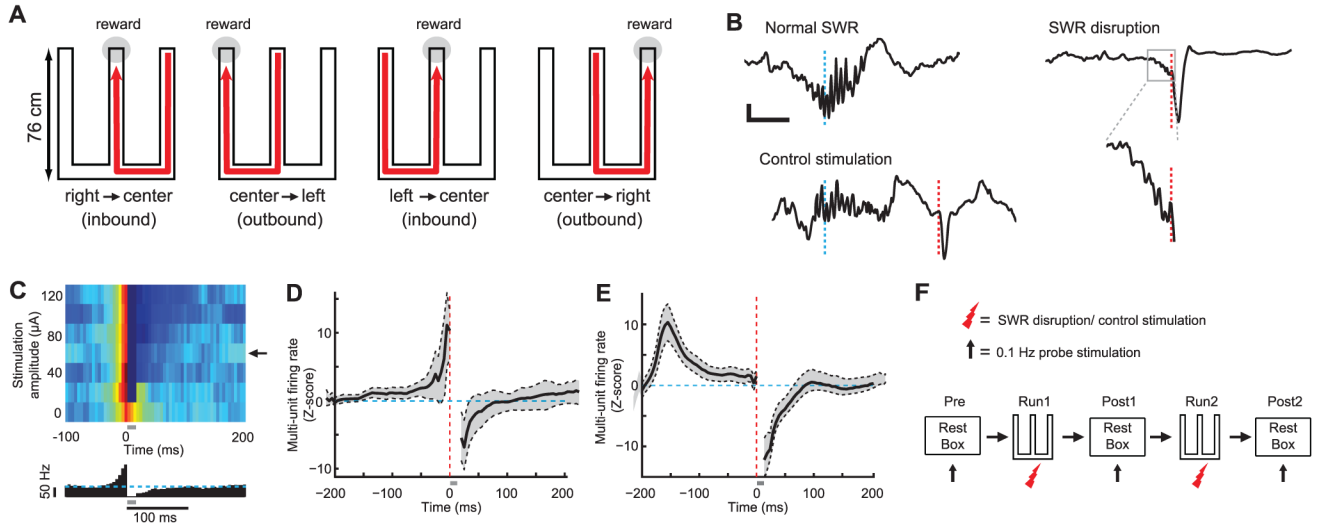30. Murray AJ, et al. Nat Neurosci. 2011; 14:297. [PubMed: 21278730]

Fig. 1.

Experimental design and SWR disruption during behavior. (**A**) Schematic illustrating the W-track task. (**B**) Example of a normal SWR (top left), disrupted SWR (right), and control stimulation after SWR (bottom left). Each panel shows an online detected SWR in the broadband local field potential (1 to 400 Hz). Cyan lines denote time of SWR detection; red lines denote time of vHC stimulation. The region in the gray box for the disrupted SWR is expanded below. Scale bars, 50 ms and 200 μV. (**C**) Top: Mean normalized multiunit activity (5-ms bins) versus stimulation intensity during calibration. Arrow denotes chosen amplitude. Bottom: Corresponding histogram for chosen amplitude; cyan line denotes baseline firing rate. Gray bar denotes spiking obscured by stimulation artifacts and fPSPs. (**D** and **E**) Z scores of multiunit firing rate aligned to stimulation for all sessions for the SWR disruption group (D) and the control stimulation group (E). Vertical red lines show the time of stimulation; horizontal cyan lines denote mean firing rates. (**F**) Sequence of rest and run sessions for each day.
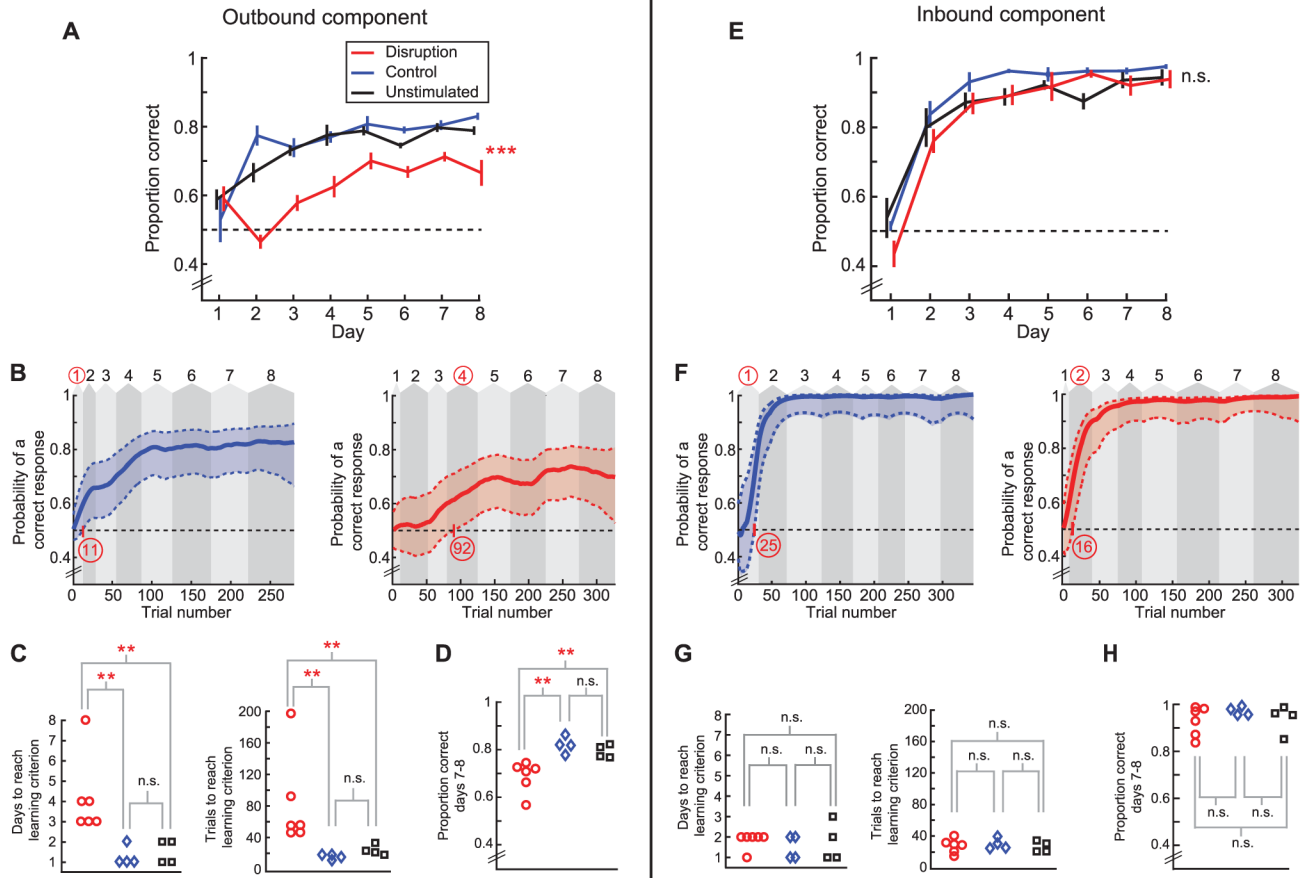
Fig. 2.
SWR disruption causes a specific impairment in the outbound, spatial working memory component of the W-track task. (**A**) Proportion correct versus day number for outbound trials. Horizontal dotted line represents chance-level performance of 0.5. (**B**) Outbound learning curves with 90% confidence intervals for a control stimulation animal (left) and a SWR disruption animal (right). Background shaded areas denote days (numbers on top). Learning trial and learning day are highlighted in red. (**C**) Outbound learning day (left) and learning trial (right) for each animal. (**D**) Average outbound performance on the last 2 days of testing (days 7 and 8). (**E** to **H**) Corresponding plots for inbound performance. *$P < 0.05$, **$P < 0.01$, ***$P < 0.001$; error bars represent SEM.
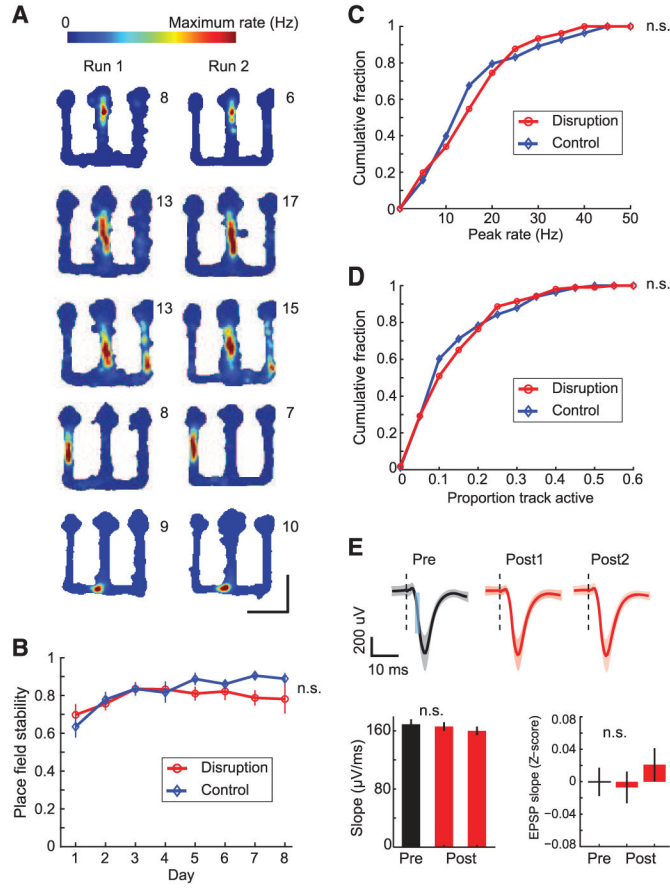
Fig. 3.
Intact place-field representations and unchanged PSPs in SWR disruption animals. (**A**) Place fields from SWR disruption animals across run sessions within a day. Color plots represent occupancy-normalized firing rates of place cells. Numbers on top right of each plot denote peak spatial firing rate. Cells are from days 2, 3, 4, 6, and 8 (top to bottom), respectively. (**B**) Place field stability across days. (**C**) Cumulative distribution function (CDF) of place field peak rates. (**D**) CDF of place field sizes. (**E**) Evoked field responses during rest sessions. Top: Example showing mean evoked field PSPs during rest sessions in a single day in a SWR disruption animal. Shaded areas represent SEM. Dotted black lines indicate time of stimulation. Slopes of field PSPs were measured in the 1.5- to 2-ms window illustrated by cyan area in the left panel. Bottom: Slopes for the example above (left), and *Z* scores of field PSP slopes in the pre and post rest sessions for the SWR disruption group (right).

Fig. 4.

Reactivation during SWRs in rest periods after behavior is intact. (**A**) Examples of reactivation from SWR disruption animals. Left: Place fields for cells during run sessions. Center: Cross-correlations for the cell pairs during run. Right: Cross-correlations during SWRs in rest periods. (**B**) Reactivation strength versus place field overlap for all cell pairs in the two groups ($n = 183$ pairs for the SWR disruption group; $n = 145$ pairs for the control stimulation group). Line represents best linear fit corresponding to the *r* value. (**C**) Mean SWR rate during the pre and post rest sessions. Error bars represent SEM.